Numerical Investigation of Wake Flow Control by a Splitter Plate

Woe-Chul Park* and Hiroshi Higuchi**

(*Received April 8, 1997*)

Unsteady separated flow around a square cylinder is simulated by using vortex tracing method to investigate the wake flow control by a splitter plate attached to the base of a bluff body. The numerical method is evaluated with selected numerical parameters for the case without the splitter plate. Then the method is applied to computations for different splitter plate lengths. Instantaneous flow patterns are scrutinized to see how the splitter plate affects the vortex formation behind the body and the downstream shedding. It is confirmed that the drag and the frequency are significantly reduced by the splitter plate, suppressing vortex shedding in the wake.

Key Words: Unsteady Separated Flow, Bluff Body, Splitter Plate, Vortex Method, Wake Flow control

Nomenclature

C_D : Drag coefficient, drag/$0.5\rho U_0^2$h
C_L : Lift coefficient, lift/$0.5\rho U_0^2$h
C_P : Pressure coefficient
d : Distance from vortex to wall
D_o : Merging parameter
h : Side of square cylinder
L : Length of splitter plate
n : Unit normal vector
N_F : Number of free vortices
N_V : Number of vortices
N_W : Number of wall points
R_o : Distance from creation point to wall
St : Strouhal number, fh/U_o(f is vortrex shedding frequency)
Δs : Segment length between two neighboring wall points
t : Time
T : Nondimensional time, tU_o/h
ΔT : Time step, $\Delta tU_o/h$
$\boldsymbol{U}$: Velocity vector (U, V)
U_o : Freestream velocity
V_o : Merging tolerance
Z : Complex position $(x+iy)$
Γ : Circulation
ρ : Fluid density
σ : Radius of vortex blob
ψ : Stream function
ω : Vorticity

* Dept. of Safety Engng, Pukyong National University
** Dept. of Mechanical, Aerospace and Manufacturing Engng, Syracuse University, U. S. A.

1. Introduction

Reduction of drag and suppression of vibration of a bluff body have been an important subject in many areas. Drag and vibration of a bluff body which moves in a fluid or is submerged in a flow are closely related to the vortex formation and shedding in the wake of the body. Among methods to control the vortex shedding a simple one is attaching a splitter plate to the base of the body. Experimental studies on such a flow control by a splitter plate have been carried out by Roshko(1954), Grove et al. (1964), Bearman (1965), Gerrad(1966), Bearman and Trueman (1972), Apelt et al. (1973), Mansingh and Oosthuizen(1990), and Hasan and Budair(1994). However, not many numerical studies have been reported up to date. Park and Higuchi(1988) computed flow around rectangular cylinders with a split-

ter plate of length L/h=5.0 by using a vortex method. Cete and Unal(1992) applied a vortex method with conformal mapping-transformation technique to a circular cylinder for splitter plates of L/h=0~2.0. Arai and Saitoh(1992) investigated effects of gap between a square cylinder and a splitter plate of L/h=1.0 using the finite difference method. Park(1993) simulated to see the effect of the splitter plate length on drag reduction for the square cylinder with L/h=0~5.0.

For better understanding of the roles of the splitter plate on wake flow control, it is necessary to investigate the aerodynamic aspects such as vortex formation and shedding and the reduction of the drag and Strouhal number by a splitter plate in a wide range of its length. In the present study, flow around a square cylinder was computed to investigate the vortex formation, its growth in the wake, and the downstream shedding for different splitter plate lengths.

Drag of a square cylinder remains nearly constant in a wide range of Reynolds number. The vortex tracing method(Spalart and Leonard, 1982), one of the inviscid vortex methods, has shown good results in simulations for the square (e. g., Park and Higuchi, 1988). The method does not require either conformal mapping or taking care of the Kutta condition on introduction of nascent vortices to the fluid. Because of these advantages the vortex tracing method has been chosen in the present study. First the vortex method is briefly introduced, and numerical parameters in the method were tested for rectangular cylinders without the splitter plate. The results with selected parameters were compared with measurements. Then the method was applied to the calculation for different splitter plate lengths. Flow patterns, drag and lift coefficients, and Strouhal numbers are presented.

2. Numerical Method

Figure 1 is a square cylinder with a splitter plate attached to the base in a uniform flow field. There are bound vortices at the creation points, j, j+1, ⋯ in the fluid around the square cylinder

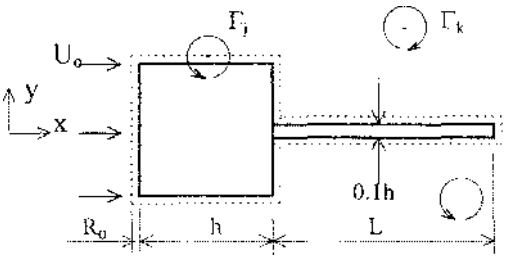

Fig. 1 A square cylinder with splitter plate.

with the circulation of Γ_j, Γ_{j+1}, ⋯, and free vortices k, k+1, ⋯, with Γ_k, Γ_{k+1}, ⋯ The surface of the cylinder and splitter plate is discretized into NW wall points.

The flow field is expressed by the following potential equation from the continuity equation and the definition of vorticity,

$$\nabla^2\psi=-\omega \tag{1}$$

The boundary condition on the body surface is,

$$\boldsymbol{U}\cdot\boldsymbol{n}=0 \tag{2}$$

and, far from the body the following is satisfied ;

$$U=U_o \tag{3}$$

Note that the computational domain is infinite and no boundary conditions on inflow and outflow are required.

The stream function at a wall point is the sum of the stream functions of all vortices, that is,

$$\psi=\sum_{j=1}^{N_v}\psi_j \tag{4}$$

and the stream function at the i-th wall point is written as

$$\begin{aligned}\psi_i=&Im[Z_{wi}(U-iV)]\\&-\frac{1}{4\pi}\sum_{j=1}^{N_w}\Gamma_j\ln(|Z_{wi}\\&-Z_{cj}|^2+\sigma^2)\\&-\frac{1}{4\pi}\sum_{k=1}^{N_f}\Gamma_k\ln(Z_{wi}-Z_k|^2+\sigma^2)\end{aligned} \tag{5}$$

The first term on the right hand side represents the stream function due to freestream, and the second and the third are due to the bound vortices and free vortices, respectively. In this study, $U=U_0$, and $V=0$ since the angle of attack is zero. Γ_j and Γ_k are the circulation of the bound vortices and the free vortices. Z_w, Z_c and Z_k are the

complex positions of the wall points, creation points and free vortices, respectively. In this equation the only unknown is Γ_j. The stream function for the wall point $i+1$ can be written in the same manner by replacing the subscript i with $i+1$.

Since the body surface is a streamline, the stream functions at the two neighboring wall points i and $i+1$ are the same, that is,

$$\psi_i = \psi_{i+1} \tag{6}$$

This yields a system of linear equations about the unknown circulation Γ_j of the bound vortices,

$$\boldsymbol{A}\Gamma = \boldsymbol{B} \tag{7}$$

where, the influence coefficient matrix $\boldsymbol{A}$ is $N_W \times N_W$, and is determined from the body configuration and positions of the vortex creation points, and the matrix $\boldsymbol{B}$ from the freestream velocity and the circulation and positions of the free vortices. $\boldsymbol{A}^{-1}$ is easily obtained by the Gauss elimination.

The vortices entered once inside the body by numerical errors are removed from computation, and their lost circulation are recovered by replacing one of the above equations with Kelvin's theorem,

$$\sum_{j=1}^{N_W} \Gamma_j = 0 \tag{8}$$

Therefore the total circulation is conserved. Solving the equations about Γ, the bound vortices are created.

Velocity of a vortex is sum of the induced velocity and freestream velocity. The velocity of the i-th vortex, induced by all other vortices, is calculated by the Biot-Savart law,

$$U_i = -\frac{1}{2\pi}\sum_{j=1}^{N_V} \Gamma_j \frac{y_j - y_i}{(x_j - x_i)^2 + (y_j - y_i)^2 + \sigma^2} \tag{9}$$

$$V_i = \frac{1}{2\pi}\sum_{j=1}^{N_V} \Gamma_j \frac{x_j - x_i}{(x_j - x_i)^2 + (y_j - y_i)^2 + \sigma^2} \tag{10}$$

In the method this is the most time consuming part requiring cpu time of $O(N_V^2)$.

The vortices move in the fluid with their own velocities. New position of the bound vortex is calculated by the Euler scheme,

$$Z^{n-1} = Z^n + \boldsymbol{U}^n \Delta t/N \tag{11}$$

and that of the free vortex by the Adams-Bashforth scheme,

$$Z^{n-1} = Z^n + (1.5\boldsymbol{U}^n - 0.5\boldsymbol{U}^{n-1})\Delta t/N \tag{12}$$

Here N is an integer number, and n denotes the computational sequence. Instead of Δt, a smaller time step $\Delta t/N$ was used to reduce numerical errors in convection of the vortices. These integrations are accurate of $O(\Delta t)$ and $O(\Delta t^2)$, respectively.

Since N_w new vortices are created at every Δt, the total number of vortices rapidly increases. To control the total number of vortices a vortex merging device(Spalart and Leonard, 1982) is used. Two vortices indexing i and j merge when

$$\frac{|\Gamma_i \Gamma_j|}{|\Gamma_i + \Gamma_j|[(D_o + d_i)(D_o + d_j)]^{1.5}} < V_o \tag{13}$$

With this ad-hoc merging device, the vortices merge more likely when their circulation is small and they rotate in the same direction, and are located close each other but far from the body. The merging parameter D_o controls the density of the vortices near the body : a smaller D_o suppresses merging near the body. The merging tolerance V_o is self-adjusted to maintain the total number of vortices. When two vortices merge, the circulation and position of the new vortex are calculated by

$$\Gamma_{new} = \Gamma_i + \Gamma_j \tag{14}$$

and

$$Z_{new} = (\Gamma_i Z_i + \Gamma_j Z_j)/(\Gamma_i + \Gamma_j) \tag{15}$$

so the circulation and linear impulse are conserved.

The instantaneous drag coefficient C_D and lift coefficient C_L are calculated from the circulation and positions of the vortices as

$$C_D = \frac{1}{\Delta t U_o^2 h/2}\left\{\left(\sum_{i=1}^{N_v}\Gamma_i y_i\right)^{n+1} - \left(\sum_{i=1}^{N_v}\Gamma_i y_i\right)^{n}\right\} \tag{16}$$

$$C_L = \frac{1}{\Delta t U_o^2 h/2}\left\{\left(\sum_{i=1}^{N_v}\Gamma_i x_i\right)^{n+1} - \left(\sum_{i=1}^{N_v}\Gamma_i x_i\right)^{n}\right\} \tag{17}$$

3. Results and Discussion

In the present study, like other vortex methods, the time-averaged drag coefficient and pressure coefficients, and the Strouhal number are compared with the available measurements to evaluate

the method. The freestream velocity U_o and the side of the square h were taken to be 1.0, respectively, for convenience. Time-averaged coefficients of drag, lift and pressure were averaged over the final 600 steps out of the total 800 time steps in each case. The Strouhal number was calculated from the time-variation of the lift coefficient during the last 512 steps.

The numerical parameters to be evaluated are N_V, N_W(or Δ_S), σ, R_o, D_o and ΔT. The values of these parameters were selected through the evaluation of the method as listed in Table 1. While testing one parameter the others remain the same as values given in the table.

Without splitter plate, 160(Δ_S/h=0.025) and 80(Δ_S/h=0.05) of the wall points N_w showed very small differences in C_D. The time-averaged drag coefficient for N_W=160 was 1.8% higher than that for N_W=80. N_W=80 was selected, which corresponds to 20 wall points each side of the square. On the surface of the splitter plate the same segment length Δ_S/h=0.05 was used.

Table 1 Selected values of numerical parameters.

Δ_S/h	0.05
R_o/h	0.0125
σ/h	0.0001
D_o/h	0.05
ΔT	0.2*
N_V	max($3N_W$, 300)

* 0.05 for convection

Figure 2 is a part of the test results for the numerical parameters N_V, σ, R_o and D_o. C_D remains nearly the same for $200 \leq N_V \leq 1200$. Computation of induced velocity requires cpu time of $O(N_V^2)$, and hence computation cost increases with N_V. $N_V=3N_W$ was selected for $N_V > 300$, but $N_V=300$ for $N_V \leq 300$. σ was tested in the range from 0.00001h to 0.001h. No significant difference in C_D was found and σ/h=0.0001 was chosen. R_o was tested for $0.005h \leq R_o \leq 0.15h$. C_D was overpredicted by about 10% when $R_o > 0.03$. R_o/h=0.0125, which is $\Delta_S/4$, was selected. The merging parameter D_o was taken to be 0.05h as recommended in Spalart and Leonard(1982).

For ΔT, among 0.05, 0.1, 0.15, 0.2, 0.3, 0.4 tested, the best periodic vortex shedding was obtained at 0.2. In convection of vortices, however, a much smaller time step ΔT=0.05 was used to reduce the numerical errors.

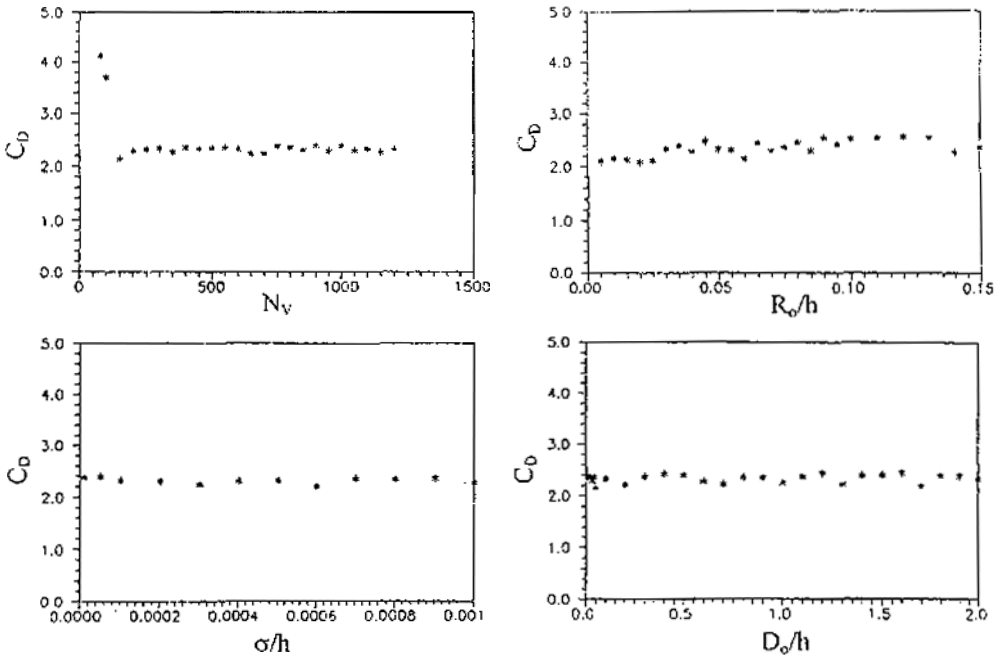

Fig. 2 Variation of C_D with numerical parameters.

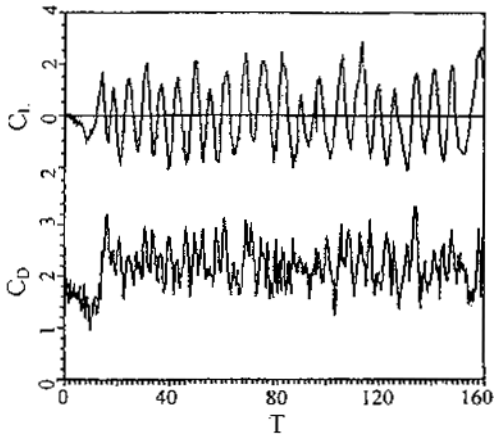

Fig. 3 Time-variation of C_L and C_D for square cylinder.

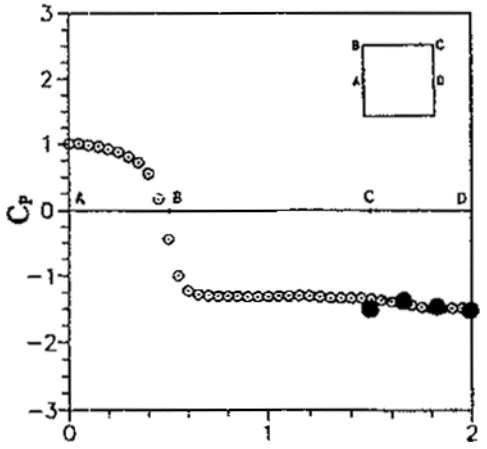

Fig. 4 Comparison of time-averaged pressure coefficient.

The calculated C_D and C_L with the selected numerical parameters are plotted in Fig. 3. For $T>20$ vortex sheds nearly regularly in the wake. The Strouhal number, which is a nondimensional vortex shedding frequency and calculated from the C_L variation, was 0.14, which agrees well with the measured values 0.14(Nagano et al., 1982) and 0.134(Hasan and Budair, 1994).

The time-averaged pressure distribution is compared in Fig. 4. The base pressure is in a good agreement. The calculated time-averaged C_D was 2.26, which also compares very well with the measured value 2.2(Bearman&Trueman, 1972).

Vortex is formed near the base of the square by the shear layers separated at the two front edges of the square. The vortices shed one by one form the Karman's vortex street. Since the splitter plate influences vortex shedding, control of the wake flow can be investigated by flow patterns. Vortex streets can be shown by streaklines, but the sequential procedure of formation and shedding of vortices is better expressed by streamlines.

Figures 5~8 show flow evolutions by streamlines for the splitter plate lengths $L/h=0$, 1.0, 3.2 and 4.4. Without splitter plate(Fig. 5) the streamlines show rolling-up of the upper shear layer to the base, and a vortex rotating counter-clockwise is formed near the base at $T=42$, but a clockwise vortex is formed by the lower shear layer at $T=44$. Vortex formation near the base at $T=46$ and 48 is nearly opposite to that at $T=42$ and $T=44$. The Karman's vortex street is clearly shown.

Figure 6 depicts streamlines for $L/h=1.0$. Comparing with $L/h=0$ in Fig. 5, it can be seen that the separated shear layers are not rolled up close to the base of the body, but the splitter plate forces that at the end of the plate where vortices are formed. Blocking by the splitter plate lowers the velocity near the base and this results in a sharp decrease in drag of the body.

The computed drag coefficient for $L/h=0$ was 2.26, and 1.80 for $L/h=1.0$, that shows about 20% reduction in drag by the splitter plate of $L/h=1.0$ as compared in Table 2. The measured drag coefficients are not available except for $L/h=0$ and 5.0. The streamlines also show much lower vortex shedding frequency.

Separation of the separated upper and lower shear layers by a longer splitter plate yields a

Table 2 Comparison of drag coefficients.

L/h	Drag coefficient(C_D)	
	Experiment*	Present study
0.0	2.20	2.26
1.0	-	1.80
2.0	-	1.62
5.0	1.34	1.47

* Bearman & Trueman(1972)

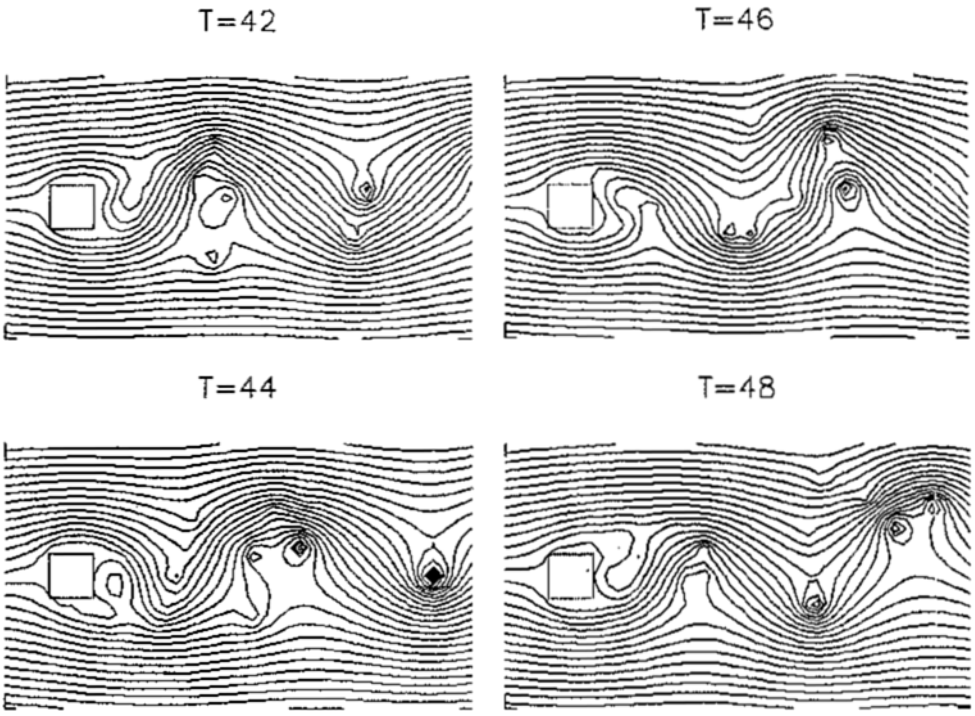

Fig. 5 Instantaneous flow patterns for $L/h=0$.

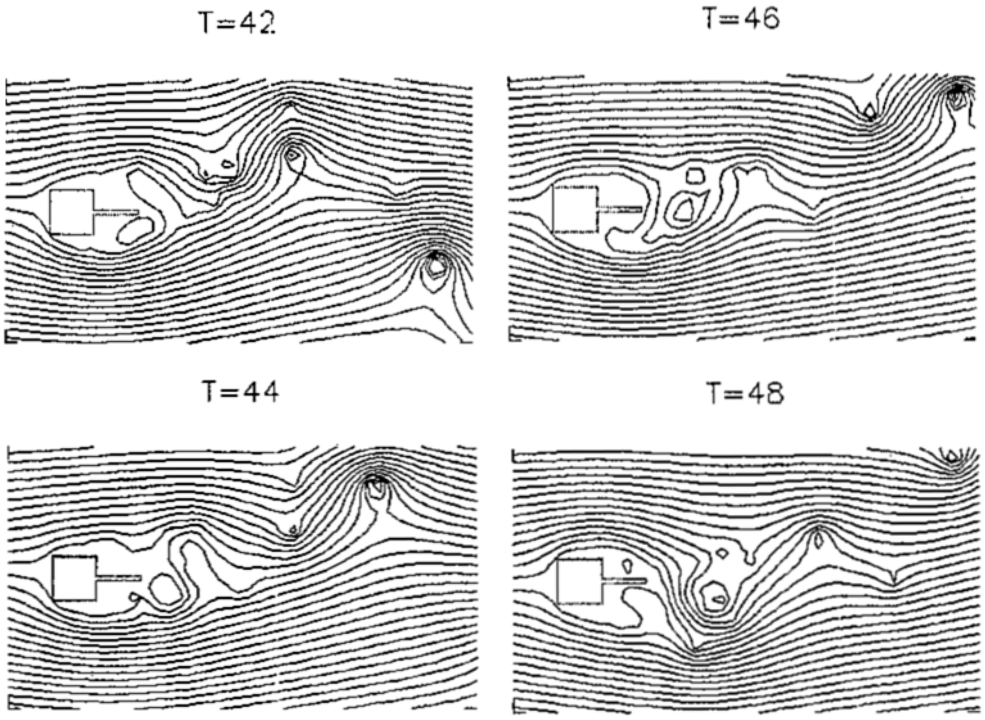

Fig. 6 Instantaneous flow patterns for $L/h=1.0$.

Table 3 Comparison of Strouhal numbers.

L/h	Strouhal Number(St)	
	Experiment*	Present study
0.0	0.134**	0.140
1.0	0.116	0.080
2.0	0.071	0.053
5.0	0.10	-

* Hasan & Budair(1994)

** 0.14(Nagano et al., 1982)

larger low velocity region behind the body, but the roles of the plate to reduces drag and vortex shedding frequency becomes smaller. Figures 7 and 8 are the flow patterns for $L/h=3.2$ and 4.4, respectively. The splitter plate suppress the interaction of the separated shear layers until vortices reach the end of the plate. Vortices are formed separately above and below the plate. C_D were respectively 1.53 for $L/h=3.2$ and 1.65 for $L/h=4.4$.

The Strouhal number is compared in Table 3. The vortex shedding frequency is also significantly reduced by the splitter plate. The Strouhal numbers are underpredicted except for $L/h=0$. It was difficult to calculate the Strouhal number because of irregular C_L variation and not enough computation steps for $L/h>3.0$.

4. Conclusions

Flow around a square cylinder with a splitter plate was computed using vortex tracing method for different aplitter lengths to investigate the wake flow control by plate. The instantaneous flow patterns showed that the splitter plate blocks the roll-up of the separated shear layers close to the base of the body, and lowers the velocity near the base, the drag of the body, and the vortex shedding frequency. Interaction of the separated shear layers was delayed until the end of the plate. Because of this, shorter splitter plates were more sensitive to wake flow control by forming smaller low velocity regions behind the body. Both drag and Strouhal number were significantly reduced

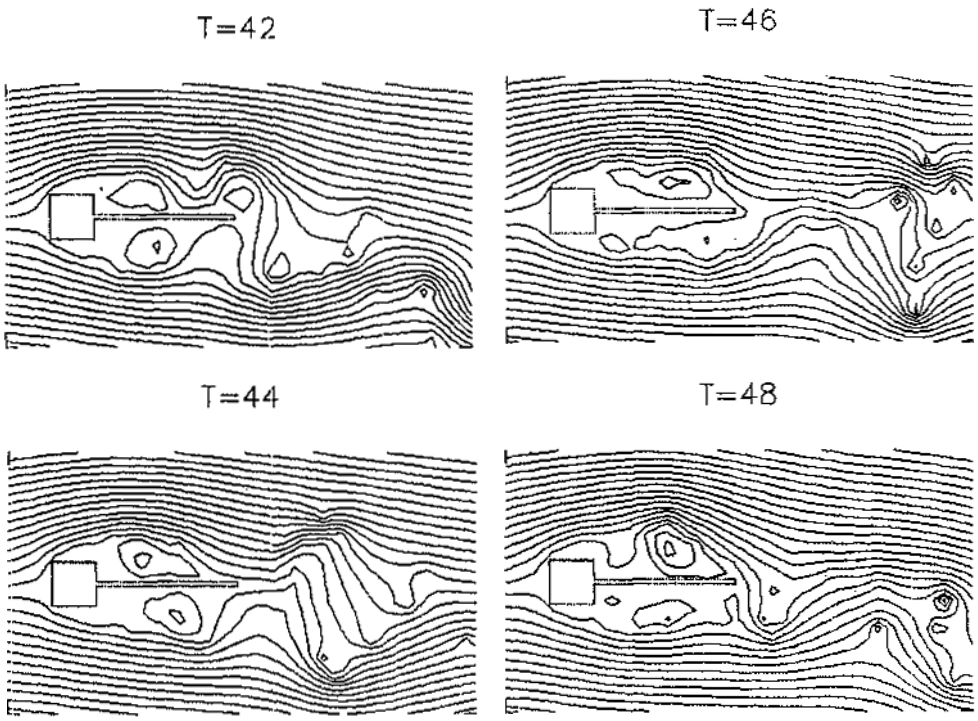

Fig. 7 Instantaneous flow patterns for $L/h=3.2$.

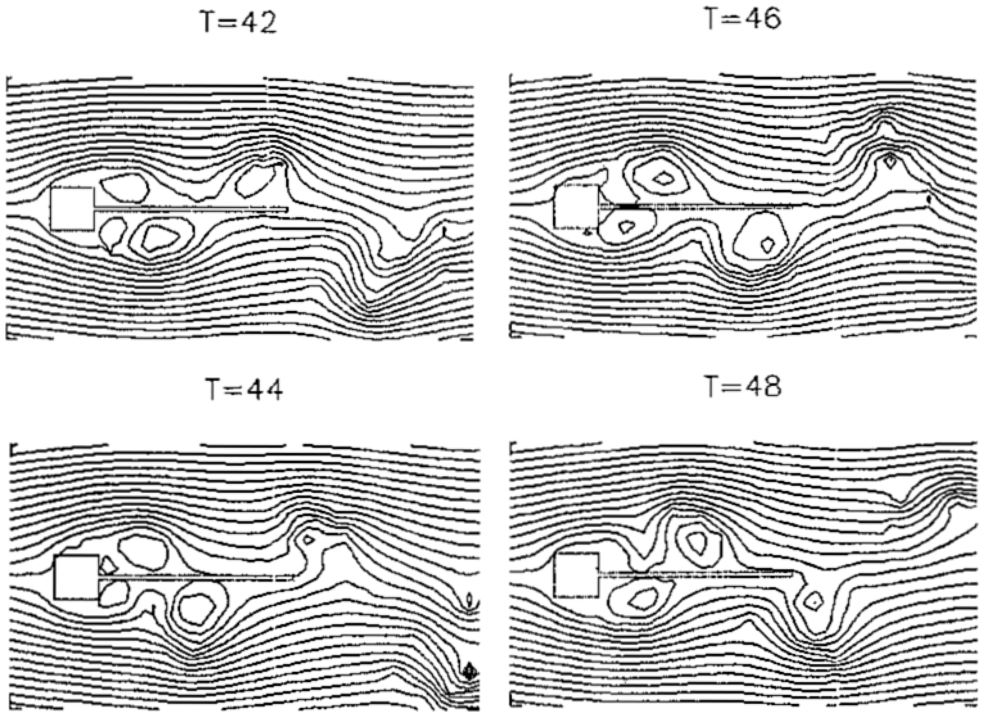

Fig. 8 Instantaneous flow patterns for $L/h=4.4$.

by suppressing the vortex shedding in the wake.

References

Apelt, C. J., West, G. S. and Szewczyk, A. A., 1973, "The Effects of Wake Splitter Plates on the Flow Past a Circular Cylinder in the Range $10^4 < Re < 5\times10^4$," *J. Fluid Mech.,* Vol. 61, pp. 187~198.

Arai, N. and Saitoh, S., 1992, "A Numerical Investigation of Flow Around a Square Section Cylinder Mounted with a Splitter Plate," *Proc. 1st European CFD Conference, CFD 2,* Vol. 1, pp. 331~336.

Bearman, P. W., 1965, "Investigation of the Flow Behind a Two-Dimensional Model with a Blunt Trailing Edge and Fitted Splitter Plates," *J. Fluid Mech.,* Vol. 21, pp. 241~255.

Bearman, P. W. and Trueman, D. M., 1972, "An Investigation of the Flow around Rectangular Cylinders," *Aeronaut. Quart.,* August, pp. 229~237.

Cete, A. R. and Unal, M. F., 1992, "Effects of Splitter Plate on Wake Formation from a Circular Cylinder: a Discrete Vortex Simulation," *Proc. 1st European CFD Conference, CFD '92,* Vol. 1, pp. 349~356.

Gerrad, J. H., 1966, "The Mechanics of the Formation Region of Vortices Behind Bluff Bodies," *J. Fluid Mech.,* Vol. 25, pp. 401~413.

Grove, A. S., Shair, F. H., Peterson, E. E. and Acrivos, A., 1964, "An Experimental Investigation of the Steady Separated Flow Past a Circular Cylinder," *J. Fluid Mech.,* Vol. 19, pp. 60~80.

Hasan, M. A. Z. and Budair, M. O., 1994, "Role of Splitter Plates in Modifying Cylinder Wake Flows," *AIAA J.,* Vol. 32, No. 10, pp 1992~1998.

Mansingh, V. and Oosthuizen, P. H., 1990, "Effects of Splitter Plates on the Wake Flow Behind a Bluff Body," *AIAA J.,* Vol. 28, No. 5, pp. 778~783.

Nagano, S., Naito, M. and Takata, H., 1982, "A Numerical Analysis of Two-Dimensional Flow Past a Rectangular Prism by a Discrete Vortex Model," *Computers and Fluids,* Vol. 10, No. 4,

pp. 243~259.

Park, W. C., 1993, "Effect of the Length of a Splitter Plate on Drag Reduction," *Trans. KSME,* Vol. 17, No. 11, pp. 2809~2815(in Korean).

Park, W. C. and Higuchi, H., 1988, "Numerical Simulations of the Flow Past Two-Dimensional Bluff Bodies with Vortex Tracing Method," *Univ. of Minnesota Supercomputer Inst, UMSI 88/99. AIAA Paper* 90-1499.

Roshko, A., 1954, "On the Drag and Shedding Frequency of Two-Dimensional Bluff Bodies," *NACA TN* 3169.

Spalart, P. R. and Leonard, A., 1981, "Computation of Separated Flows by a Vortex Tracing Algorithm," *AIAA Paper* 81-1246.